

## **CHARACTERIZATION OF REBARS ANCHORAGE IN UHPC**

**Ekkehard Fehling (1), Paul Lorenz (2)**

(1) Concrete Structures, University Kassel.

### **Abstract**

To understand the behaviour of reinforced ultra high performance concrete structures, it is important to understand the bond behaviour of rebars in UHPC. Therefore test series were conducted to determine the influence of the main parameters, especially to get basic information for the development of design rules for anchorage of rebars in UHPC. Due to the filigree character of UHPC structures the concrete cover and the mode of failure are the main parameters in these investigations. If fibres are added, it is important to know how they influence the bond behaviour and if they can replace a transverse reinforcement. The anchorage specimens showed different failure modes as well as combinations thereof. The results will be compared with those of pull-out tests to weigh the respective parameters. The main objective is to determine the necessary anchorage length of non-prestressed rebars in fine grained UHPRC for practical dimensions of building members used in the construction industry subject to the parameters concrete cover and fibre efficiency.

### **Résumé**

Pour comprendre le comportement des structures armées en béton à ultra-hautes performances (BUHP), il faut comprendre l'adhérence des armatures dans le BUHP. Des essais ont donc été conduits pour déterminer l'influence des principaux paramètres, en particulier pour obtenir l'information nécessaire à l'élaboration de règles de conception pour l'ancrage des barres dans le BUHP. Compte tenu de la minceur des ouvrages en BUHP l'enrobage et le mode de rupture ont été les principaux paramètres étudiés. En présence d fibres, il faut connaître leur influence sur l'adhérence et leur capacité éventuelle à remplacer le ferrailage transversal. Les corps d'épreuve pour essais d'ancrage dans les deux premières séries d'essais ont mis en évidence les différents modes de rupture et leur combinaison. On compare les résultats avec ceux des essais d'arrachement de la troisième série pour analyser le poids respectif des paramètres. Le but principal est de déterminer la longueur de scellement minimale pour les armatures passives dans du BFUP sans gros granulats, en vue d'un dimensionnement pratique dans l'industrie, en fonction des paramètres que constituent l'enrobage et l'efficacité des fibres.

## 1. INTRODUCTION

UHPC exhibits high values of compressive strengths near those of structural steel, which enables reducing cross sections and the use of less material. In terms of reinforcement corrosion, the high packing density and the high resistance against ingress of fluids and gases allows markedly smaller concrete covers. At the same time, minimum concrete cover requirements must be observed in order to ensure a secure anchorage. Due to the load transfer from the ribbed bar along the ribs into the concrete, diagonal struts are formed, which are balanced by a tensile ring. Failure of the tensile ring results in formation of splitting cracks, which negatively affect the bond capacity. Due to the fact that the increase of the tensile strength in comparison with that of NSC is subproportional lower than the increase in compression strength, the focus must be placed on tensile failure. It is known that fibres have positive effects on the tensile failure characteristics.

For NSC various anchorage failure modes were examined by Eligehausen [1]. These are pull-out, pry-out, splitting as well as combinations of these individual modes. Each mode can be influenced by different parameters, for example confinement, the addition of fibres, relative rib area, concrete cover, casting direction etc. For this reason, the relevant parameters must be determined to design anchorage lengths for the ULS. These will be examined within the framework of a project funded by the German Research Foundation (DFG).

## 2. OWN TESTS ON ANCHORAGE OF REBARS IN UHPC

Three different series were examined. In all series the ribbed bar on which the bond behaviour was to be observed was BSt 500 S (nominal yield stress  $f_{yk} = 500$  MPa) with a diameter of  $d_s = 12$  mm. The parameters under investigation were embedded length  $l_b$ , concrete cover  $c$  and fibre content  $\rho_f$ . In the first and second series the specimens consisted of panels with constant length and width (see Fig. 1 and 3).

### 2.1 First test series

The main goal of this series was to see the relationship between failure mode, the concrete cover and the bond length.

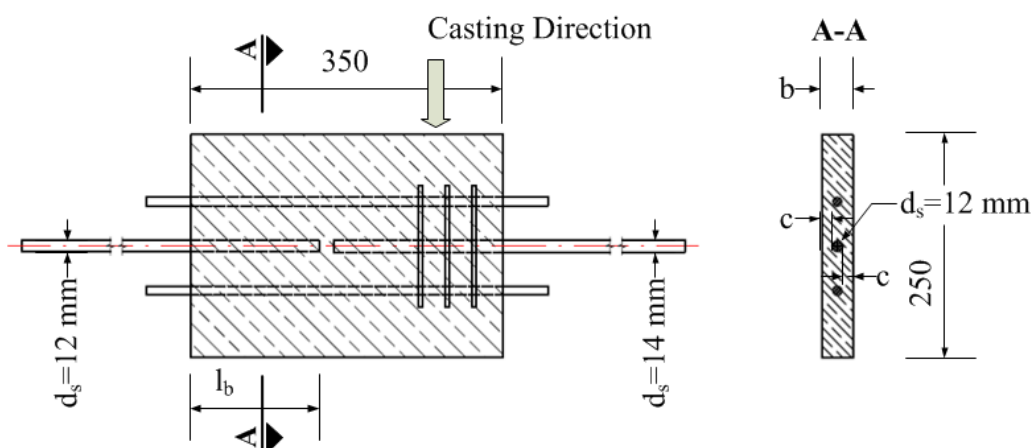


Figure 1: Specimen principle for ribbed bar Pull-Out with variable embedded lengths and concrete covers (dimensions in mm)

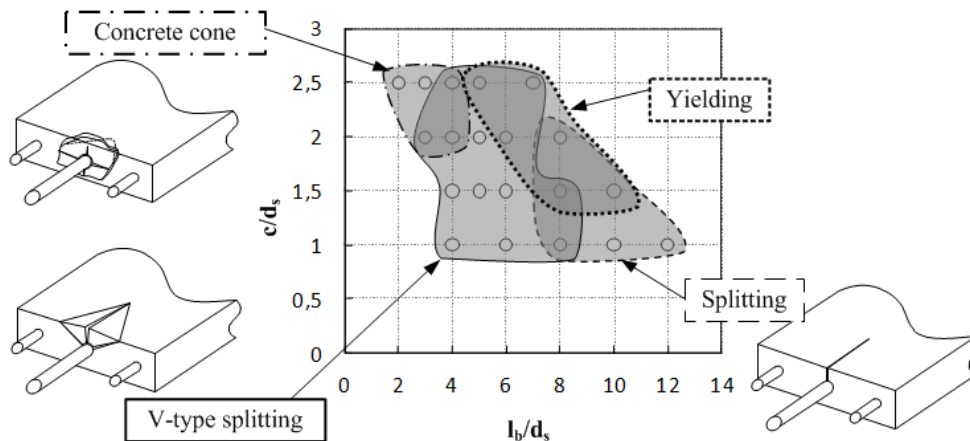


Figure 2: Investigated parameters ( $l_b$ ,  $c$  with  $d_s = 12$  mm) and the major failure modes of the test specimens in the first series.

The test setup, the test procedure and the results are described in detail in [2]. Parameters with variation of value were concrete cover  $c$  and embedded length  $l_b$ . Tab. 1 gives a survey of the main test results for the examined parameters. In the following the results are summarized briefly. The average bond strength was calculated with  $\tau_{bm,max} = \sigma_{s,max} / (4 l_b / d_s)$ . The dimensions of the specimen can be seen in Fig. 1. A fibre reinforced fine grained UHPC (M3Q according to DFG Priority Program 1182 in [3]) with a maximum aggregate size of 0.5 mm has been used. The steel fibres had a tension strength of about 2.4 GPa and a  $l_f / d_f$ -ratio of  $13 \text{ mm} / 0.19 \text{ mm} = 68$  and the content  $\rho_f$  was 1.5 % by volume. The formwork was stripped after 48 hours. Afterwards heat treatment at a temperature of 90 °C was applied to the specimens for 48 hours. The concrete compressive strength was 170 MPa at the age of 28 days.

Table 1: Loaded side steel stresses  $\sigma_{s,max}$  and average bond strength  $\tau_{bm,max}$  at maximum load for the specimens of the first test series ( $\rho_f = 1.5$  % by volume with  $l_f / d_f = 68$ ).

max. steel stress $\sigma_{s,max}$ , bond strength $\tau_{bm,max}$ in [MPa]			Bond length ratio ( $l_b/d_s$ )								
			2.0	3.0	4.0	5.0	6.0	7.0	8.0	10.0	12.0
Concrete cover ratio ( $c/d_s$ )	2.5	$\sigma_{s,max}$	325	436	536	624	-	560	-	-	-
		$\tau_{bm,max}$	40.6	36.3	33.5	31.2	-	20.0	-	-	-
	2.0	$\sigma_{s,max}$	-	362*	438*	558*	582	-	677	-	-
		$\tau_{bm,max}$	-	30.2	27.4	27.9	24.2	-	21.1	-	-
	1.5	$\sigma_{s,max}$	-	-	397	489	512	-	639	674	-
		$\tau_{bm,max}$	-	-	24.8	24.5	21.3	-	20.0	16.9	-
	1.0	$\sigma_{s,max}$	-	-	284	-	374	-	517	516	507
		$\tau_{bm,max}$	-	-	17.8	-	15.6	-	16.2	12.9	10.6

\* - Tests with same parameters were also conducted in the second test series

Different basic failure modes were observed: There was concrete cone failure, v-type splitting or splitting and yielding of reinforcement (see Fig. 2). In most cases, mixed failure modes were observed. For this reason, failure modes were evaluated on the basis of the failure pattern. The relationship between the observed failure modes, the concrete cover and the embedded length is shown in Fig. 2. It can be seen that there are smooth transitions between the different failure modes.

For  $c / d_s \geq 7.0$  and the small concrete cover the bond strength values are shown in grey because here a “zipper-effect” was observed (see Tab. 1).

## 2.2 Second test series

The main goal of this series was to see the influence of transverse reinforcement. In this series the same geometry of the specimen and the fabrication process was used as in the first one. The UHPC mixture was identical but with different steel fibres. The fibres used here had a  $l_f / d_f$ -ratio of  $17\text{mm} / 0.175\text{mm} = 98$  and the content was 1.0 % by volume.

Leutbecher presented in [4] an equation for calculating the fibre efficiency.

$$\sigma_{cf0} = \eta \cdot g \cdot \rho_f \cdot \tau_f \cdot l_f / d_f \quad (1)$$

Where  $\eta$  = coefficient of fibre orientation,  $g$  = coefficient of fibre efficiency,  $\rho_f$  = fibre content,  $\tau_f$  = average bond stress,  $l_f$  = length of the fibre and  $d_f$  = diameter of the fibre.

Assuming that the product of the parameters  $\eta$ ,  $g$  where the same as in first series, the fibre content in the second series was adjusted in dependence of the  $l_f / d_f$ -ratio to have about the same fibre efficiency. The compressive strength in the second series was 210 MPa.

In contrast to the first series, a transverse reinforcement was applied here. Two types were used: 1 stirrup or 2 bars per specimen. Both of them were placed at the first third of the bond length (see Fig. 3). The transverse reinforcement had a diameter of 6 mm. The test setup and the test procedure were the same as in the first series. The main results can be seen in Tab. 3.

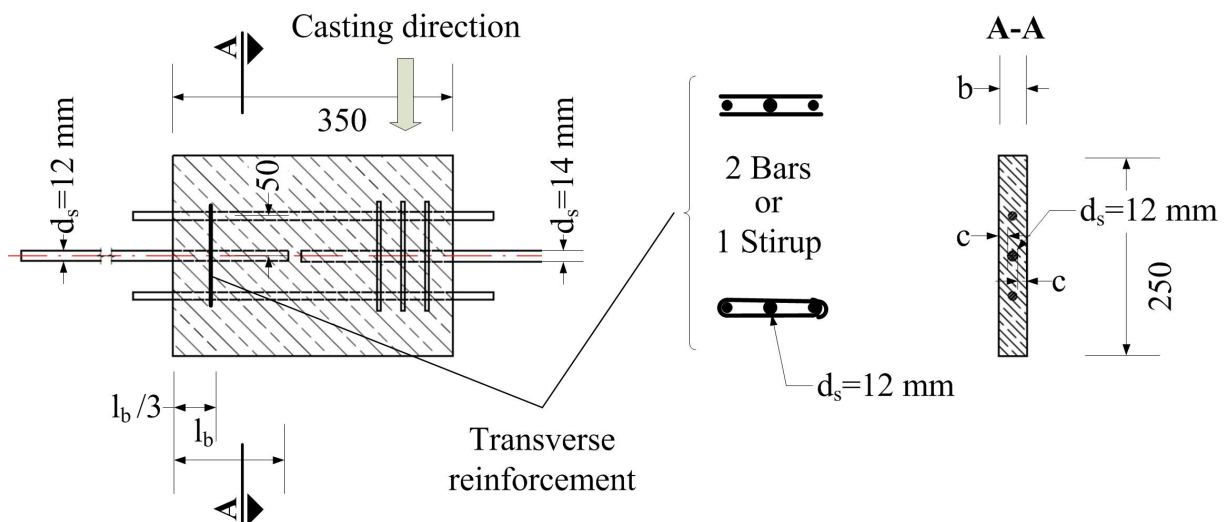


Figure 3: Specimen principle for ribbed bar Pull-Out with varying embedded lengths, concrete covers and transverse reinforcement (dimensions in mm).

The parameters  $c / d_s = 2.0$  and  $l_b / d_s = 3.0$  until 5.0 were the same in the first and second test series (see Tab. 1 and 3). For these parameters, the maximum possible loaded side steel stresses in the second test series were smaller than in the first. One possible reason could be a smaller fibre efficiency i.e. a smaller fibre bond strength.

Table 2: Loaded side steel stresses  $\sigma_{s,max}$  and the average bond strength  $\tau_{bm,max}$  at maximum load for the specimens of the second test series ( $\rho_f = 1.0$  % by volume with  $l_f / d_f = 98$ ).

max. steel stress $\sigma_{s,max}$ , bond strength $\tau_{bm,max}$ in [MPa]		Bond length ratio ( $l_b/d_s$ )				
		2,0	3,0	4,0	5,0	
Concrete cover ratio ( $c/d_s$ )	2.5 <sup>b</sup>	$\sigma_{s,max}$	289	374	433	556
		$\tau_{bm,max}$	36,1	31,2 (87%)	27,1 (91%)	27,8 (97%)
	2,0	$\sigma_{s,max}$	266	357*	389*	512*
		$\tau_{bm,max}$	33,3	29,8 (100%)	24,3 (100%)	25,6 (100%)
	1.5 <sup>s</sup>	$\sigma_{s,max}$	187	278	412	554
		$\tau_{bm,max}$	23,4	23,2	25,8 (117%)	27,7 (123%)
	1,0 <sup>b</sup>	$\sigma_{s,max}$	108	183	308	-
		$\tau_{bm,max}$	13,5	15,3	19,3 (122%)	-

\* - Tests with same parameters were also conducted in the first test series

() - Effectiveness of transverse reinforcement

<sup>b</sup> - transverse reinforcement with two bars

<sup>s</sup> - transverse reinforcement with one stirrup

If we compare the bond strength in the first test series for  $l_b / d_s = 3.0$  between  $c / d_s = 2.5$  and  $c / d_s = 2.0$  there is an improvement of 20 % ( $36.3 / 30.2 = 1.20$ ). In the second test series this improvement is only 5 % ( $31.2 / 29.8 = 1.05$ ) even though a transverse reinforcement with two bars is used. By dividing the improvement ratio due to transverse reinforcement from the second test series through the one due to concrete cover from the first test series we get a value of effectiveness for the transverse reinforcement. For this case it is 87%. For the other cases it is shown in Tab. 2 in brackets. These values show a negative influence of the transverse reinforcement for concrete cover and bond length parameters with concrete cone failure modes ( $c / d_s = 2.5$  and  $l_b / d_s \leq 4.0$  in Fig. 2). For the failure mode v-type splitting the transverse reinforcement had positive influences ( $c / d_s \leq 1.5$  and  $l_b / d_s \geq 4.0$  in Fig. 2).

### 2.3 Third test series

This series was examined to see the influence of fibres. The second target was to see if there is a large difference between the slip on the loaded and the unloaded side of the ribbed bar respectively to find out if the whole bond length is activated.

#### Experimental program

The specimens consisted of a block with constant length, width and height. Two bars were placed in this block. One with an embedded length of  $3.5 d_s$  and one with an embedded length of  $5.0 d_s$  (see Fig. 4). To investigate the influence of the fibre content three blocks were made with a fibre content of 0.5, 1.0 and 1.5 % by vol. (see Tab. 3). The type of fibres, the heat

treatment and the UHPC mixture was the same as in the second test series. The compression strength was about 210 MPa. The ribbed bar on which the bond behaviour was to be observed was a cold-rolled BSt 500 S with a diameter of  $d_s = 12$  mm, a yield strength of  $f_{y0.1} \approx 535$  MPa and tension strength between 580 and 610 MPa.

Table 3: Investigated parameters in the third series and the test denomination

	$\rho_f = 0.5$ % by volume	$\rho_f = 1.0$ % by volume	$\rho_f = 1.5$ % by volume
$l_b / d_s = 3.5$	S3VF05L35	S3VF10L35	S3VF15L35
$l_b / d_s = 5.0$	S3VF05L50	S3VF10L50	S3VF15L50

As Fig. 4 shows, the rebar had a defined bond length ( $5.0 d_s$  and  $3.5 d_s$ ). The rest of the embedded length was taped twice with a foam tape and, therefore, free of bond. The maximum possible undisturbed outbreak body had a diameter of 300 mm. And so the maximum undisturbed angle  $\alpha$  of the outbreak body was about  $25^\circ$ .

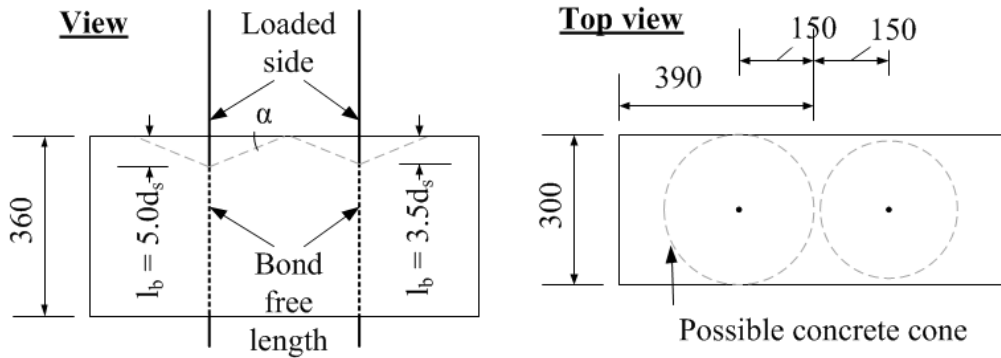


Figure 4: Specimen principle for ribbed bar Pull-Out with variable bond lengths and fibre content (dimensions in mm).

### Test setup and test procedure

After the installation of the specimen in the machine the LVDTs were applied. The load application on the rebar was done by a clamping device and the specimen was fixed on the ground. The force was measured by a cell and was applied in a displacement controlled way with a rate of 0.1 mm/sec.

There were three groups of LVDTs. The groups A, B and C were placed on the loaded side and the group D was placed on the unloaded side (see Fig. 6). The steel strain on the bar was obtained from the elongation  $\Delta l_B$  as measured by the LVDT-Group B with a measurement length  $l_B$  (see Fig. 6) by  $\varepsilon_s = \Delta l_B / l_B$ . The slip between the steel and the concrete was measured indirectly by the LVDT Group A. Here the measurement-length was  $l_A$  and the measured elongation was  $\Delta l_A = s + l_A \cdot \varepsilon_s$ . The slip was calculated from the measured values (see Eq. 2) using the assumption that the strains within  $l_A$  and  $l_B$  are identical. This assumption is valid for elastic behaviour but not after onset of yielding.

$$s_A = \Delta l_A - l_A \cdot \Delta l_B / l_B \quad (2)$$

After occurrence of an outbreak body, the LVDT-Group A could only measure the local slip. Therefore, the additional Group C was installed. This Group was related on a point outside the outbreak body and therefore it measured indirectly the actual slip or the deformation of the outbreak body. The calculation of this slip  $s_B$  was carried out analogously to the previous one in Eq. 2 by using the elongation  $\Delta l_C$  instead of  $\Delta l_B$  and the measurement length  $l_C$  instead of  $l_B$ . The Group D was installed at the unloaded side to measure here directly the slip and/or the crack opening of the outbreak body.

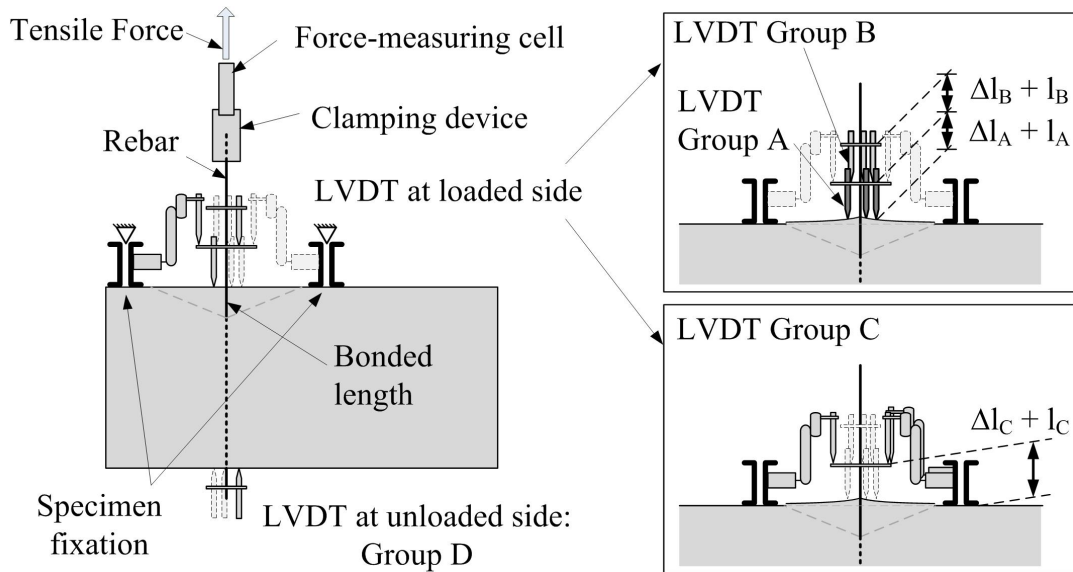


Figure 6: LEFT: Specimen in experimental setup  
 RIGHT TOP and BOTTOM: LVDTs arrangement at loaded side.

## Results

During the test different slips were measured and different failure modes were observed. The steel stress-slip relationships of the individual tests are shown in Fig. 7. After reaching the yield strength (two-point-dash line), the slip could be determined only qualitatively and should therefore be regarded with caution. Three different graphs per diagram show different types of slip or deformation. The letter A, C or D after “S\_” indicates the group of LVDTs which was used to calculate the slip (see LVDT Groups in Fig. 6).

The main parameters can be derived from the test denomination. „V12“ represents an anchorage of a bar diameter of 12 mm. The two-digit number without a decimal point after the letter “F” indicates the fibre content in % by vol. and the number after “L” the anchorage ratio (see Fig. 7).

Because the slip  $S_C$  was referred to a point outside the concrete cone, it measured a shear deformation of the concrete cone related to the fixation points. These deformations were not measured by the slip  $S_D$ . So the slip  $S_C$  is always greater than the slip  $S_D$  at same steel stresses. The difference between these slips is getting smaller with decreasing steel stress in the post peak-behaviour because the shear deformation and the deformation of the fixation parts decrease.

For all fibre contents and bond lengths it can be said that the whole bond length was activated, because at the unloaded side a significant slip  $S_D$  has been observed.

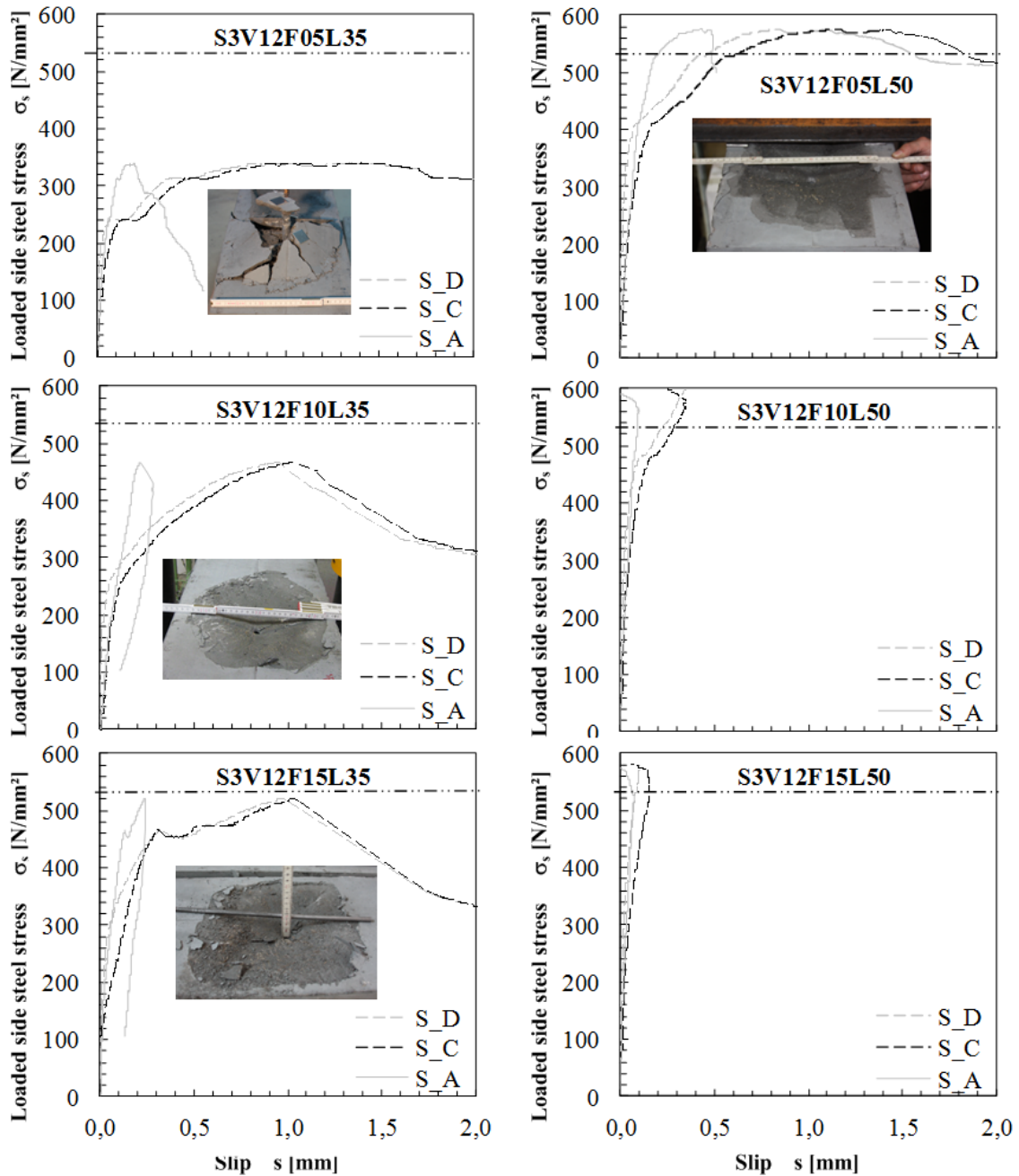


Figure 7: Steel stress-slip (LVDT Group A,C,D) for different  $\rho_f$  (TOP: 0.5 %, MID:1.0 %, BOTTOM: 1.5 %) and different  $l_b$  (LEFT:  $l_b = 3,5d_s$ , RIGHT:  $l_b = 5,0d_s$ )

#### Results for $l_b = 3.5 d_s$

For an embedded length of  $3.5 d_s$  the steel stresses were under the yield strength (see Fig. 7). Further for a fibre content of 0.5 % by vol. the slip S\_A increased after reaching the maximum steel stress. On the other hand for the same embedded length and a fibre content of 1.0 and 1.5 % by vol. this slip decreased after reaching the maximum steel stress. That indicates that the failure mode was a different one. In the first case after the test there was no concrete cone. There were a lot of radial cracks (see picture in Fig. 7). In the second and third

case there was only a concrete cone which had no visible radial cracks. This cone remained at the end of the test on the ripped bar. After removing the bar with the cone the outbreak body was visible (see picture in Fig. 7). For both fibre contents the shape of the concrete cone was similar. But the maximum steel stress was higher (about 530 MPa).

#### Results for $l_b = 5.0 d_s$

For an embedded length of  $5.0 d_s$ , a fibre content of 1.0 and 1.5 % by vol. the steel failure was decisive (see Fig. 7). During and after the test there was no concrete cone visible on the surface of the specimen. For a fibre content of 1.5 % by vol. there was definitely no concrete cone failure. But in Fig. 7 for a fibre content of 1.0 % by vol. occurred a difference between the slip  $S_A$  and  $S_C$  at a steel stress of 480 MPa. That means that there was a cone which was simply not visible. For a fibre content of 0.5 % by vol. there was a concrete cone failure because the slip  $S_A$  increases with the slip  $S_D$  after the onset of yielding. The cone remained on the bar. The size of the cone is shown in Fig. 7.

Table 4: Loaded side steel stresses  $\sigma_{s,max}$  and the average bond strength  $\tau_{bm,max}$  at maximum load for the specimens of the third test series ( $l_f / d_f = 98$ ).

max. steel stress and bond strength [MPa]		$l_b / d_s = 3.5$	$l_b / d_s = 5.0$
$\rho_f = 0.5$ % by volume	$\sigma_{s,max} / \tau_{bm,max}$	340 / 24.3	575 / 28.8
$\rho_f = 1.0$ % by volume	$\sigma_{s,max} / \tau_{bm,max}$	467* / 33.3	615* / 30.8
$\rho_f = 1.5$ % by volume	$\sigma_{s,max} / \tau_{bm,max}$	520 / 37.1	581 / 29.1

\* - Tests with same parameters were also conducted in the first test series

#### Comparing first and third series

The loaded side steel stress at maximum load increases less than proportional with the fibre content respectively with the fibre efficiency. This is due to different failure modes that must be considered.

If one compares the results from the first test series with them of the third test series the following can be noted. In the first test series for  $c = 2.5 d_s$ , and  $l_b = 3.0 d_s$  respectively  $4.0 d_s$ , there was a maximum steel stress at the loaded side of 436 MPa respectively 536 MPa (see Tab. 1). By linear interpolation a steel stress of 486 MPa is expected for  $l_b = 3.5 d_s$ . In the third series at a fibre content of 1.0 % by vol. and  $l_b = 3.5 d_s$  the maximum steel stress was 467 MPa (see Fig. 7 and Tab. 4). That means that the greater concrete cone with a diameter of about  $16 d_s$  (20 cm in Fig. 5) in contrast to  $6 d_s$  ( $= 2c + 1 d_s$ ) led to lower maximum steel stress. In the first test series for  $c = 2.5 d_s$  and  $l_b = 5.0 d_s$  there was a maximum steel stress at the loaded side of 624 MPa (see Tab. 1). In the third series for  $l_b = 5.0 d_s$  and a fibre content of 1.0 % by vol. the maximum steel stress 615 MPa was reached. In both cases the steel was yielding. If we compare the maximum steel stresses for  $l_b = 5.0 d_s$  at  $\rho_f = 0.5$  % by vol. and  $l_b = 3.5 d_s$  at  $\rho_f = 1.5$  % by vol., it can be noted that a 30 % shorter bond length could not be compensated by a three times higher fibre content.

### 3. CONCLUSIONS

As expected, it could be observed that an increase of the concrete cover leads to a disproportionately lower increase of the average bond strength at maximum load (see Tab. 1).

For a fibre content of 1.0 % by vol. and concrete covers  $c < 2.5 d_s$  splitting occurs only at bond length  $l_b \geq 8 d_s$ . Only in this cases the “zipper-effect” has to be considered which means that the activated bond length at maximum load could be smaller than the full bond length (see section 2.1).

For concrete cone failure, the maximum steel stress increases not in same way for small concrete covers of  $c = 2.0 d_s$  or  $2.5 d_s$  (see Tab. 1) as for large concrete cover  $c = 7.5 d_s$  (see Tab. 4, excluding yielding) when increasing the bond length  $l_b$ . So, it is not possible to define one definite relationship between the bond length  $l_b$  and the maximum steel stress for this failure mode.

For a fibre content of 1.0 % by vol., a bond length  $l_b \leq 8 d_s$ , and a concrete cover of  $c = 1.0 d_s$  or  $1.5 d_s$ , the average bond strength  $\tau_{bm,max}$  is independent from the bond length (see Tab. 1). It seems that for this failure mode an unique bond stress-slip law is valid. However, if the failure mode changes to splitting (for  $l_b > 8 d_s$  and  $c = 1.0 d_s$ ), there is a decrease in the bond strength due to the splitting crack. This means that the local bond stress-slip law highly depends on the width of the local splitting crack and the tensile stress in the crack respectively. As a matter of fact, the rebar could not be fully activated up to yield stress at  $c = 1.0 d_s$  and a fibre content of 1.0 % by vol. even for bond length of  $l_b = 12 d_s$ .

No positive influence of transverse reinforcement could be observed in the case of concrete cone failure ( $c = 2.5 d_s$  and  $l_b \geq 3.0 d_s$ ). This may be explained by the fact that the transverse reinforcement was too short (see Fig. 3) to intersect the cone shaped crack. For the v-type splitting failure, applying transverse reinforcement showed a positive influence.

At very large concrete covers, a combination of concrete cone failure and splitting cracking occurs. The small slip difference between the loaded and unloaded side in series 3 (see Fig. 7) indicates a dominant influence of the concrete cone failure. Increasing the fibre content results in a disproportionately lower increase of bond strength or of maximum steel stress at the loaded side. To activate higher values of bond strength, i.e. to get shorter bond length, high fibre contents are needed that may be uneconomically.

## REFERENCES

- [1] Eligehausen, R & Mallée, R & Silva; J.F. 2006. Anchorage in Concrete Construction. Berlin: Ernst & Sohn.
- [2] Fehling, E. & Lorenz, P. & Leutbecher, T. Experimental Investigations on Anchorage of Rebars in UHPC Proc. of 3rd in-tern. symp. on UHPC and nanotechnology for high performance construction materials, Kassel, 7-9 March 2012.
- [3] DFG SPP 1182: DFG Schwerpunktprogramm, Nachhaltiges Bauen mit ultrahochfestem Beton
- [4] Leutbecher, T. & Fehling, E. 2012. Tensile Behaviour of Ultra-High-Performance Concrete Reinforced with Reinforcing Bars and Fibres-Minimizing Fibre Content. ACI Structural Journal 109-S24 pp. 253-263
- [5] fib 2000. Bond of reinforcement in concrete. State of the art report. Lausanne: International Federation for Structural Concrete.